

KO codes: inventing nonlinear encoding and decoding for reliable wireless communication via deep-learning

Anonymous Authors¹

Abstract

Landmark codes underpin reliable physical layer communication, e.g., Reed-Muller, BCH, Turbo, LDPC and Polar codes: each is a linear code and represents a mathematical breakthrough. The impact on humanity is huge: each of these codes has been used in global wireless communication standards (satellite, WiFi, cellular). Reliability of communication over the classical additive white Gaussian noise (AWGN) channel enables benchmarking and ranking of the different codes. In this paper, we construct KO codes, a computationally efficient family of deep-learning driven (encoder, decoder) pairs that outperform the state-of-the-art reliability performance on the standardized AWGN channel. KO codes represent important firsts: (a) the first nonlinear family of codes; (b) the first codes to beat state-of-the-art algebraic codes in the challenging short-medium block length regime on the AWGN channel. Our key technical innovation that renders this possible is design of a novel family of neural architectures inspired by the computation tree of the Kronecker Operation (KO) central to Reed-Muller and Polar codes. These architectures pave way for the discovery of a much richer class of hitherto unexplored nonlinear algebraic structures.

1. Introduction

Physical layer communication underpins the information age (WiFi, cellular, cable and satellite modems). Codes, composed of encoder and decoder pairs, are the basic mathematical objects enabling reliable communication: encoder maps original data bits into a longer sequence, and decoders map the received sequence to the original bits. Reliability is precisely measured: bit error rate (BER) measures the

fraction of input bits that were incorrectly decoded; block error rate (BLER) measures the fraction of times at least one of the original data bits was incorrectly decoded.

Landmark codes include Reed-Muller (RM), BCH, Turbo, LDPC and Polar codes (Richardson & Urbanke, 2008): each is a linear code and represents a mathematical breakthrough discovered over a span of six decades. The impact on humanity is huge: each of these codes has been used in global communication standards over the past six decades. These codes essentially operate at the information-theoretic limits of reliability over the AWGN channel, when the number of information bits is large, the so-called “large block length” regime. In the small and medium block length regimes, the state-of-the-art codes are *algebraic*: encoders and decoders are invented based on specific linear algebraic constructions over the binary and higher order fields and rings. Especially prominent algebraic codes are the RM and Polar families, whose encoders are recursively defined as Kronecker products of a simple linear operator and constitute the state of the art in small-to-medium block length regimes.

Inventing new codes is a major intellectual activity both in academia and the wireless industry; this is driven by emerging practical applications, e.g., low block length regime in Internet of Things (Ma et al., 2019). The core challenge is that the space of codes is very vast and the sizes astronomical; for instance a rate 1/2 code over even 100 information bits involves designing 2^{100} codewords in a 200 dimensional space. Computationally efficient encoding and decoding procedures are a must, apart from high reliability. Thus, although a random code is information theoretically optimal, neither encoding nor decoding is computationally efficient. The mathematical landscape of computationally efficient codes has been plumbed over the decades by some of the finest mathematical minds, resulting in two distinct families of codes: *algebraic codes* (RM, Polar, BCH – focused on properties of polynomials) and *graph codes* (Turbo, LDPC – based on sparse graphs and statistical physics). The former is deterministic and involves discrete mathematics, while the latter harnesses randomness, graphs, and statistical physics to behave like a pseudorandom code. A major open question is the invention of new codes, and especially fascinating would be a family of codes outside of these two

¹Anonymous Institution, Anonymous City, Anonymous Region, Anonymous Country. Correspondence to: Anonymous Author <anon.email@domain.com>.

Preliminary work. Under review by the International Conference on Machine Learning (ICML). Do not distribute.

classes.

Our major result is the invention of a new family of codes, called KO codes, that have features of both code families: they are nonlinear generalizations of the Kronecker operation underlying the algebraic codes (RM, Polar) parameterized by neural network; the parameters are learnt in an end-to-end training paradigm in a data driven manner. Deep learning (DL) has transformed several domains of human endeavor that have traditionally relied heavily on mathematical ingenuity, e.g., game playing (AlphaZero (Silver et al., 2018)), biology (AlphaFold (Senior et al., 2019)), and physics (new laws (Udrescu & Tegmark, 2020)). Our results can be viewed as an added domain to the successes of DL in inventing mathematical structures.

A linear encoder is defined by a *generator matrix*, which maps information bits to a codeword. The RM and the Polar families construct their generator matrices by recursively applying the Kronecker product operation to a simple two-by-two matrix and then selecting rows from the resulting matrix. The careful choice in selecting these rows is driven by the desired algebraic structure of the code, which is central to achieving the large *minimum* pairwise distance between two codewords, a hallmark of the algebraic family. This encoder can be alternatively represented by a computation graph. The recursive Kronecker product corresponds to a complete binary tree, and row-selection corresponds to freezing a set of leaves in the tree, which we refer to as a “Plotkin tree”, inspired by the pioneering construction in (Plotkin, 1960).

The Plotkin tree skeleton allows us to tailor a new neural network architecture: we expand the algebraic family of codes by replacing the (linear) Plotkin construction with a non-linear operation parametrized by neural networks. The parameters are discovered by training the encoder with a matching decoder, that has the matching Plotkin tree as a skeleton, to minimize the error rate over (the unlimited) samples generated on AWGN channels.

Algebraic and the original RM/Polar codes promise a large worst-case pairwise distance (Alon et al., 2005). This ensures that RM/Polar codes achieve capacity in the large block length limit (Arikan, 2009; Kudekar et al., 2017). However, for short block lengths, they are too conservative as we are interested in the average-case reliability. This is the gap KO codes exploit: we seek a better average-case reliability and not the minimum pairwise distance.

Figure 1 illustrates the gain for the example of RM(9, 2) code. Using the Plotkin tree of RM(9, 2) code as a skeleton, we design the KO(9, 2) code architecture and train on samples simulated over an AWGN channel. We discover a novel non-linear code and a corresponding efficient decoder that improves significantly over the RM(9, 2) code baseline.

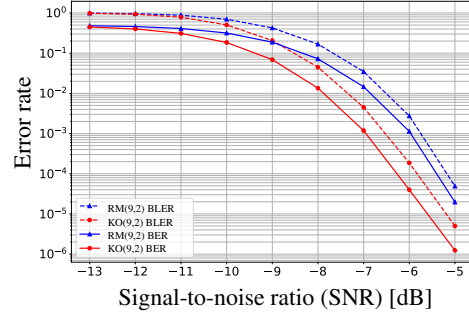


Figure 1. KO(9, 2), discovered by training a neural network with a carefully chosen architecture in §3, significantly improves upon state-of-the-art RM code RM(9, 2) both in BER and BLER (for both codes, the code block length is $2^9 = 512$ and the number of transmitted message bits is $\binom{9}{0} + \binom{9}{1} + \binom{9}{2} = 55$).

Analyzing the pairwise distances between two codewords reveals a surprising fact. The histogram for KO code nearly matches that of a random Gaussian codebook. The skeleton of the architecture from an algebraic family of codes, the training process with a variation of the stochastic gradient descent, and the simulated AWGN channel have worked together to discover a novel family of codes that harness the benefits of both algebraic and pseudorandom constructions.

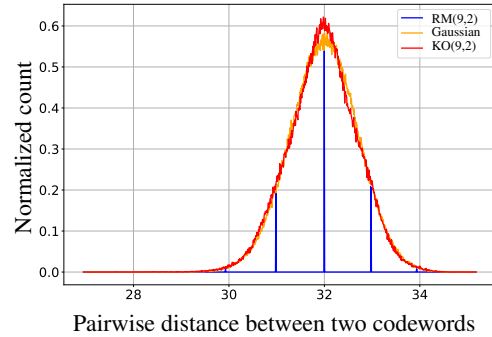


Figure 2. Histogram of pairwise distances between codewords of the KO(9, 2) code shows a staggering resemblance of that of the Gaussian codebook, unlike the classical Reed-Muller code RM(9, 2).

In summary, we make the following contributions: We introduce novel neural network architectures for the (encoder, decoder) pair that generalizes the Kronecker operation central to RM/Polar codes. We propose training methods that discover novel non-linear codes when trained over AWGN and provide empirical results showing that this family of non-linear codes improves significantly upon the baseline code it was built on (both RM and Polar codes). Interpreting the pairwise distances of the discovered codewords reveals that a KO code mimics the distribution of codewords from the random Gaussian codebook, which is known to

be reliable but computationally challenging to decode. The decoding complexities of KO codes are $O(n \log n)$ where n is the block length, matching that of efficient decoders for RM and Polar codes.

2. Problem formulation and background

We formally define the channel coding problem and provide background on Reed-Muller codes, the inspiration for our approach. Our notation is the following. We denote Euclidean vectors by bold face letters like \mathbf{m} , \mathbf{L} , etc. For $\mathbf{L} \in \mathbb{R}^n$, $\mathbf{L}_{k:m} \triangleq (L_k, \dots, L_m)$. If $\mathbf{v} \in \{0, 1\}^n$, we define the operator $\oplus_{\mathbf{v}}$ as $\mathbf{x} \oplus_{\mathbf{v}} \mathbf{y} \triangleq \mathbf{x} + (-1)^{\mathbf{v}} \mathbf{y}$.

2.1. Channel coding

Let $\mathbf{m} = (m_1, \dots, m_k) \in \{0, 1\}^k$ denote a block of *information/message bits* that we want to transmit. An encoder $g_{\theta}(\cdot)$ is a function parametrized by θ that maps these information bits into a binary vector \mathbf{x} of length n , i.e. $\mathbf{x} = g_{\theta}(\mathbf{m}) \in \{0, 1\}^n$. The rate $\rho = k/n$ of such a code measures how many bits of information we are sending per channel use. These codewords are transformed into real (or complex) valued signals, called modulation, before being transmitted over a channel. For example, Binary Phase Shift Keying (BPSK) modulation maps each $x_i \in \{0, 1\}$ to $1 - 2x_i \in \{\pm 1\}$ up to a universal scaling constant for all $i \in [n]$. Here, we do not strictly separate encoding from modulation and refer to both binary encoded symbols and real-valued transmitted symbols as *codewords*.

Upon transmission of this codeword \mathbf{x} across a noisy channel $P_{Y|X}(\cdot|\cdot)$, we receive its corrupted version $\mathbf{y} \in \mathbb{R}^n$. The decoder $f_{\phi}(\cdot)$ is a function parametrized by ϕ that subsequently processes the received vector \mathbf{y} to estimate the information bits $\hat{\mathbf{m}} = f_{\phi}(\mathbf{y})$. The closer $\hat{\mathbf{m}}$ is to \mathbf{m} , the more reliable the transmission. An error metric, such as Bit-Error-Rate (BER) or Block-Error-Rate (BLER), gauges the performance of the encoder-decoder pair (g_{θ}, f_{ϕ}) . Note that BER is defined as $\text{BER} \triangleq (1/k) \sum_i \mathbb{P}[\hat{m}_i \neq m_i]$, whereas $\text{BLER} \triangleq \mathbb{P}[\hat{\mathbf{m}} \neq \mathbf{m}]$.

The design of good codes given a channel and a fixed set of code parameters (k, n) can be formulated as:

$$(\theta, \phi) \in \arg \min_{\theta, \phi} \text{BER}(g_{\theta}, f_{\phi}), \quad (1)$$

which is a joint classification problem for k binary classes, and we train on the surrogate loss of cross entropy to make the objective differentiable. While classical optimal codes such as Turbo, LDPC, and Polar codes all have *linear* encoders, appropriately parametrizing both the encoder $g_{\theta}(\cdot)$ and the decoder $f_{\phi}(\cdot)$ by neural networks (NN) allows for a much broader class of codes, especially non-linear codes. However, in the absence of any structure, NNs fail to learn non-trivial codes and end up performing worse than simply

repeating each message bit n/k times (Kim et al., 2018; Jiang et al., 2019b).

A fundamental question in machine learning for channel coding is thus: how do we design architectures for our neural encoders and decoders that give the appropriate inductive bias? To gain intuition towards addressing this, we focus on Reed-Muller (RM) codes. In §3, we present a novel family of non-linear codes, *KO codes*, that strictly generalize and improve upon RM codes by capitalizing on their inherent recursive structure. Our approach seamlessly generalizes to Polar codes, explained in §5.

2.2. Reed-Muller (RM) codes

We use a small example of RM(3,1) and refer to Appendix D for the larger example in our main results.

Encoding. RM codes are a family of codes parametrized by a variable size $m \in \mathbb{Z}_+$ and an order $r \in \mathbb{Z}_+$ with $r \leq m$, denoted as RM(m, r). It is defined by an *encoder*, which maps binary information bits $\mathbf{m} \in \{0, 1\}^k$ to codewords $\mathbf{x} \in \{0, 1\}^n$. RM(m, r) code sends $k = \sum_{i=0}^r \binom{m}{i}$ information bits with $n = 2^m$ transmissions. The *code distance* measures the minimum distance between all (pairs of) codewords. Table 1 summarizes these parameters.

Code length	Code dimension	Rate	Distance
$n = 2^m$	$k = \sum_{i=0}^r \binom{m}{i}$	$\rho = k/n$	$d = 2^{m-r}$

Table 1. Parameters of an RM(m, r) code

One way to define RM(m, r) code is via the recursive application of a *Plotkin construction*. The basic building block is a mapping Plotkin : $\{0, 1\}^{\ell} \times \{0, 1\}^{\ell} \rightarrow \{0, 1\}^{2\ell}$, where

$$\text{Plotkin}(\mathbf{u}, \mathbf{v}) = (\mathbf{u}, \mathbf{u} \oplus \mathbf{v}), \quad (2)$$

with \oplus representing a coordinate-wise XOR and (\cdot, \cdot) denoting concatenation of two vectors (Plotkin, 1960).

In view of the Plotkin construction, RM codes are recursively defined as a set of codewords of the form:

$$\text{RM}(m, r) = \{(\mathbf{u}, \mathbf{u} \oplus \mathbf{v}) : \mathbf{u} \in \text{RM}(m-1, r), \mathbf{v} \in \text{RM}(m-1, r-1)\}, \quad (3)$$

where RM($m, 0$) is a repetition code that repeats a single information bit 2^m times, i.e., $\mathbf{x} = (m_1, m_1, \dots, m_1)$. When $r = m$, the full-rate RM(m, m) code is also recursively defined as a Plotkin construction of two RM($m-1, m-1$) codes. Unrolling the recursion in Eq. (3), a RM(m, r) encoder can be represented by a corresponding (rooted and binary) computation tree, which we refer to as its *Plotkin tree*. In this tree, each branch represents a Plotkin mapping of two codes of appropriate lengths, recursively applied from the leaves to the root.

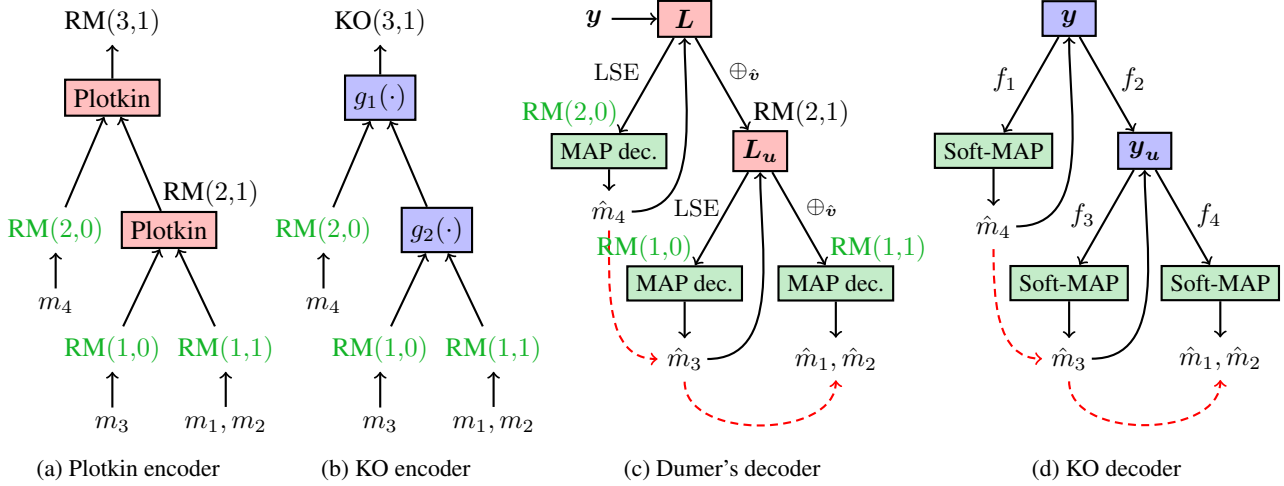


Figure 3. Plotkin trees for RM(3, 1) and KO(3, 1) codes; Leaves are shown in green. Red arrows indicate the sequential decoding order.

Figure 3a illustrates such a Plotkin tree decomposition of RM(3, 1) encoder. Encoding starts from the bottom right leaves. The leaf RM(1, 0) maps m_3 to (m_3, m_3) (repetition), and another leaf RM(1, 1) maps (m_1, m_2) to $(m_1, m_1 \oplus m_2)$ (Plotkin mapping of two RM(0, 0) codes). Each branch in this tree performs the Plotkin construction of Eq. (2). The next operation is the parent of these two leaves, which performs $\text{Plotkin}(\text{RM}(1, 1), \text{RM}(1, 0)) = \text{Plotkin}((m_1, m_1 \oplus m_2), (m_3, m_3))$ which outputs the vector $(m_1, m_1 \oplus m_2, m_1 \oplus m_3, m_1 \oplus m_2 \oplus m_3)$, which is known as RM(2, 1) code. This coordinate-wise Plotkin construction is applied recursively one more time to combine RM(2, 0) and RM(2, 1) at the root of the tree. The resulting codewords are $\text{RM}(3, 1) = \text{Plotkin}(\text{RM}(2, 1), \text{RM}(2, 0)) = \text{Plotkin}((m_1, m_1 \oplus m_2, m_1 \oplus m_3, m_1 \oplus m_2 \oplus m_3), (m_4, m_4, m_4, m_4))$.

This recursive structure of RM codes (i) inherits the good minimum distance property of the Plotkin construction and (ii) enables efficient decoding.

Decoding. Since (Reed, 1954), there have been several decoders for RM codes; (Abbe et al., 2020) is a detailed survey. We focus on the most efficient one, called *Dumer's recursive decoding* (Dumer, 2004; 2006; Dumer & Shabunov, 2006) that fully capitalizes on the recursive Plotkin construction in Eq. (3). The basic principle is: to decode an RM codeword $\mathbf{x} = (\mathbf{u}, \mathbf{u} \oplus \mathbf{v}) \in \text{RM}(m, r)$, we first recursively decode the left sub-codeword $\mathbf{v} \in \text{RM}(m-1, r-1)$ and then the right sub-codeword $\mathbf{u} \in \text{RM}(m-1, r)$, and we use them together to stitch back the original codeword. This recursion is continued until we reach the leaf nodes, where we perform maximum a posteriori (MAP) decoding.

Figure 3c illustrates this decoding procedure for RM(3, 1). Dumer's decoding starts at the root and uses the soft-information of codewords to decode the message bits. Sup-

pose that the message bits $\mathbf{m} = (m_1, \dots, m_4)$ are encoded into an RM(3, 1) codeword $\mathbf{x} \in \{0, 1\}^8$ using the Plotkin encoder in Figure 3a. Let $\mathbf{y} \in \mathbb{R}^8$ be the corresponding noisy codeword received at the decoder. To decode the bits \mathbf{m} , we first obtain the soft-information of the codeword \mathbf{x} , i.e., we compute its Log-Likelihood-Ratio (LLR) $\mathbf{L} \in \mathbb{R}^8$:

$$L_i = \log \frac{\mathbb{P}[y_i | x_i = 0]}{\mathbb{P}[y_i | x_i = 1]}, \quad i = 1, \dots, 8.$$

We next use \mathbf{L} to compute soft-information for its left and right children: the RM(2, 0) codeword \mathbf{v} and the RM(2, 1) codeword \mathbf{u} . We start with the left child \mathbf{v} .

Since the codeword $\mathbf{x} = (\mathbf{u}, \mathbf{u} \oplus \mathbf{v})$, we can also represent its left child as $\mathbf{v} = \mathbf{u} \oplus (\mathbf{u} \oplus \mathbf{v}) = \mathbf{x}_{1:4} \oplus \mathbf{x}_{5:8}$. Hence its LLR vector $\mathbf{L}_v \in \mathbb{R}^4$ can be readily obtained from that of \mathbf{x} . In particular it is given by the log-sum-exponential transformation: $\mathbf{L}_v = \text{LSE}(\mathbf{L}_{1:4}, \mathbf{L}_{5:8})$, where $\text{LSE}(a, b) \triangleq \log((1 + e^{a+b}) / (e^a + e^b))$ for $a, b \in \mathbb{R}$. Since this feature \mathbf{L}_v corresponds to a repetition code, $\mathbf{v} = (m_4, m_4, m_4, m_4)$, majority decoding (same as the MAP) on the sign of \mathbf{L}_v yields the decoded message bit as \hat{m}_4 . Finally, the left codeword is decoded as $\hat{\mathbf{v}} = (\hat{m}_4, \hat{m}_4, \hat{m}_4, \hat{m}_4)$.

Having decoded the left RM(2, 0) codeword $\hat{\mathbf{v}}$, our goal is to now obtain soft-information $\mathbf{L}_u \in \mathbb{R}^4$ for the right RM(2, 1) codeword \mathbf{u} . Fixing $\mathbf{v} = \hat{\mathbf{v}}$, notice that the codeword $\mathbf{x} = (\mathbf{u}, \mathbf{u} \oplus \hat{\mathbf{v}})$ can be viewed as a 2-repetition of \mathbf{u} depending on the parity of $\hat{\mathbf{v}}$. Thus the LLR \mathbf{L}_u is given by LLR addition accounting for the parity of $\hat{\mathbf{v}}$: $\mathbf{L}_u = \mathbf{L}_{1:4} \oplus_{\hat{\mathbf{v}}} \mathbf{L}_{5:8} = \mathbf{L}_{1:4} + (-1)^{\hat{\mathbf{v}}} \mathbf{L}_{5:8}$. Since RM(2, 1) is an internal node in the tree, we again recursively decode its left child RM(1, 0) and its right child RM(1, 1), which are both leaves. For RM(1, 0), decoding is similar to that of RM(2, 0) above, and we obtain its information bit \hat{m}_3 by first applying the log-sum-exponential function on the

feature L_u and then majority decoding. Likewise, we obtain the LLR feature $L_{uu} \in \mathbb{R}^2$ for the right RM(1, 1) child using parity-adjusted LLR addition on L_u . Finally, we decode its corresponding bits (\hat{m}_1, \hat{m}_2) using efficient ML-decoding of first order RM codes (Abbe et al., 2020). Thus we obtain the full block of decoded message bits as $\hat{m} = (\hat{m}_1, \hat{m}_2, \hat{m}_3, \hat{m}_4)$.

An important observation from Dumer’s algorithm is that the sequence of bit decoding in the tree is: RM(2, 0) \rightarrow RM(1, 0) \rightarrow RM(1, 1). A similar decoding order holds for all RM(m , 2) codes, where all the left leaves (order-1 codes) are decoded first from top to bottom, and the right-most leaf (full-rate RM(2, 2)) is decoded at the end.

3. KO codes: novel neural codes

We design KO codes using the the Plotkin tree as the skeleton of a new neural network architecture, which strictly improve upon their classical counterparts.

KO encoder. Earlier we saw the design of RM codes via recursive Plotkin mapping. Inspired by this elegant construction, we present a new family of codes, called *KO codes*, denoted as KO(m, r, g_θ, f_ϕ). These codes are parametrized by a set of four parameters: a non-negative integer pair (m, r), a finite set of encoder neural networks g_θ , and a finite set of decoder neural networks f_ϕ . In particular, for any fixed pair (m, r), our KO encoder inherits the same code parameters (k, n, ρ) and the same Plotkin tree skeleton of the RM encoder. However, a critical distinguishing component of our KO(m, r) encoder is a set of encoding neural networks $g_\theta = \{g_i\}$ that strictly generalize the Plotkin mapping: to each internal node i of the Plotkin tree, we associate a neural network g_i that applies a coordinate-wise real valued non-linear mapping $(u, v) \mapsto g_i(u, v) \in \mathbb{R}^{2\ell}$ as opposed to the classical binary valued Plotkin mapping $(u, v) \mapsto (u, u \oplus v) \in \{0, 1\}^{2\ell}$. Figure 3b illustrates this for the KO(3, 1) encoder.

The significance of our KO encoder g_θ is that by allowing for general nonlinearities g_i to be learnt at each node we enable for a much richer and broader class of non-linear encoders and codes to be discovered on a whole, which contribute to non-trivial gains over standard RM codes. Further, we have the same encoding complexity as that of an RM encoder since each $g_i : \mathbb{R}^2 \rightarrow \mathbb{R}$ is applied coordinate-wise on its vector inputs. The parameters of these neural networks g_i are trained via stochastic gradient descent with a surrogate loss of the BER. See §F for experimental details.

KO decoder. Training the encoder is possible only if we have a corresponding decoder. This necessitates the need for an efficient family of matching decoders. Inspired by the Dumer’s decoder, we present a new family of *KO decoders* that fully capitalize on the recursive structure of KO

encoders via the Plotkin tree.

Our KO decoder has three distinct features: (i) Neural decoder: The KO decoder architecture is parameterized by a set of decoding neural networks $f_\phi = \{(f_{2i-1}, f_{2i})\}$. Specifically, to each internal node i in the tree, we associate f_{2i-1} to its left branch whereas f_{2i} corresponds to the right branch. Figure 3d shows this for the KO(3, 1) decoder. The pair of decoding neural networks (f_{2i-1}, f_{2i}) can be viewed as matching decoders for the corresponding encoding network g_i : While g_i encodes the left and right codewords arriving at this node, the outputs of f_{2i-1} and f_{2i} represent appropriate Euclidean feature vectors for decoding them. Further, f_{2i-1} and f_{2i} can also be viewed as a generalization of Dumer’s decoding to nonlinear real codewords: f_{2i-1} generalizes the LSE function, while f_{2i} extends the operation $\oplus_{\hat{v}}$. Note that both the functions f_{2i-1} and f_{2i} are also applied coordinate-wise and hence we inherit the same decoding complexity as Dumer’s. (ii) Soft-MAP decoding: Since the classical MAP decoding to decode the bits at the leaves is not differentiable, we design a new differentiable counterpart, the *Soft-MAP decoder*. Soft-MAP decoder enables gradients to pass through it, which is crucial for training the neural (encoder, decoder) pair (g_θ, f_ϕ) in an end-to-end manner. (iii) Channel agnostic: Our decoder directly operates on the received noisy codeword $y \in \mathbb{R}^n$ while Dumer’s decoder uses its LLR transformation $L \in \mathbb{R}^n$. Thus, our decoder can learn the appropriate channel statistics for decoding directly from y alone; in contrast, Dumer’s algorithm requires precise channel characterization, which is not usually known.

4. Main results

We train the KO encoder g_θ and KO decoder f_ϕ from §3 using an approximation of the BER loss in (1). The details are provided in Appendix F. In this section we focus on the second-order KO(8, 2) and KO(9, 2) codes.

4.1. KO codes improve over RM codes

In Figure 1, the trained KO(9,2) improves over the competing RM(9,2) both in BER and BLER. The superiority in BLER is unexpected as our training loss is a surrogate for the BER. Though one would prefer to train on BLER as it is more relevant in practice, it is challenging to design a surrogate loss for BLER that is also differentiable: all literature on learning decoders minimize only BER (Kim et al., 2020; Nachmani et al., 2018; Dörner et al., 2017). Consequently, improvements in BLER with trained encoders and/or decoders are rare. We discover a code that improves both BER and BLER, and we observe a similar gain with KO(8, 2) in Figure 4. Performance of a binarized version KO-b(8,2) is also shown, which we describe further in §B.1.

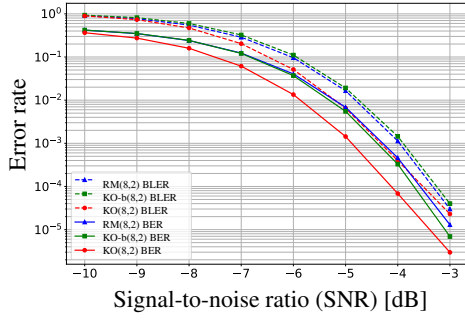


Figure 4. Neural network based KO(8, 2) and KO-b(8, 2) improve upon RM(8, 2) in BER and BLER, but the gain is small for the binarized codewords of KO-b(8, 2) (for all the codes, the code dimension is 37 and block length is 256).

4.2. Interpreting KO codes

We interpret the learned encoders and decoders to explain the source of the performance gain.

Interpreting the KO encoder. To interpret the learned KO code, we examine the pairwise distance between codewords. In classical linear coding, pairwise distances are expressed in terms of the weight distribution of the code, which counts how many codewords of each specific Hamming weight $1, 2, \dots, n$ exist in the code. The weight distribution of linear codes are used to derive analytical bounds, that can be explicitly computed, on the BER and BLER over AWGN channels (Sason & Shamai, 2006). For nonlinear codes, however, the weight distribution does not capture pairwise distances. Therefore, we explore the distribution of all the pairwise distances of non-linear KO codes that can play the same role as the weight distribution does for linear codes.

The pairwise distance distribution of the RM codes remains an active area of research as it is used to prove that RM codes achieve the capacity (Kaufman et al., 2012; Abbe et al., 2015; Sberlo & Shpilka, 2020) (Figure 5 blue). However, these results are asymptotic in the block length and do not guarantee a good performance, especially in the small-to-medium block lengths that are of interest. On the other hand, Gaussian codebooks, codebooks randomly picked from the ensemble of all Gaussian codebooks, are known to be asymptotically optimal, i.e., achieving the capacity (Shannon, 1948), and also demonstrate optimal finite-length scaling laws closely related to the pairwise distance distribution (Polyanskiy et al., 2010) (Figure 5 orange).

Remarkably, the pairwise distance distribution of KO code shows a staggering resemblance to that of the Gaussian codebook of the same rate ρ and blocklength n (Figure 5 red). This is an unexpected phenomenon since we minimize only BER. We posit that the NN training has learned to

construct a Gaussian-like codebook, in order to minimize BER. Most importantly, unlike the Gaussian codebook, KO codes constructed via NN training are fully compatible with efficient decoding. This phenomenon is observed for all order-2 codes we trained (e.g., Figure 2 for KO(9, 2)).

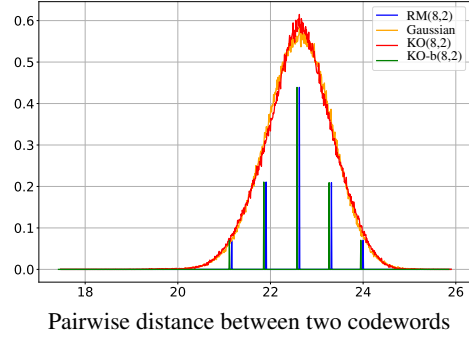


Figure 5. Histograms of pairwise distances between codewords for (8,2) codes reveal that KO(8,2) code has learned an approximate Gaussian codebook that can be efficiently decoded.

Interpreting the KO decoder. We now analyze how the KO decoder contributes to the gains in BLER over the RM decoder. Let $\mathbf{m} = (\mathbf{m}_{(7,1)}, \dots, \mathbf{m}_{(2,2)})$ denote the block of transmitted message bits, where the ordered set of indices $\mathcal{L} = \{(7, 1), \dots, (2, 2)\}$ correspond to the leaf branches (RM codes) of the Plotkin tree. Let $\hat{\mathbf{m}}$ be the decoded estimate by the KO(8, 2) decoder.

We provide Plotkin trees of RM(8,2) and KO(8,2) in Figures 12 and 13 in the appendix. Recall that for this KO(8, 2) decoder, similar to the KO(3, 1) decoder in Figure 3d, we decode each sub-code in the leaves sequentially, starting from the (7, 1) branch down to (2, 2): $\hat{\mathbf{m}}_{(7,1)} \rightarrow \dots \rightarrow \hat{\mathbf{m}}_{(2,2)}$. In view of this decoding order, BLER, defined as $\mathbb{P}[\hat{\mathbf{m}} \neq \mathbf{m}]$, can be decomposed as

$$\mathbb{P}[\hat{\mathbf{m}} \neq \mathbf{m}] = \sum_{i \in \mathcal{L}} \mathbb{P}[\hat{\mathbf{m}}_i \neq \mathbf{m}_i, \hat{\mathbf{m}}_{1:i-1} = \mathbf{m}_{1:i-1}]. \quad (4)$$

In other words, BLER can also be represented as the sum of the fraction of errors the decoder makes in each of the leaf branches when no errors were made in the previous ones. Thus, each term in Eq. (4) can be viewed as the contribution of each sub-code to the total BLER.

This is plotted in Figure 6, which shows that the KO(8, 2) decoder achieves better BLER than the RM(8, 2) decoder by making major gains in the leftmost (7, 1) branch (which is decoded first) at the expense of other branches. However, the decoder (together with the encoder) has learnt to better balance these contributions evenly across all branches, resulting in lower overall. The unequal errors in the branches

of the RM code has been observed before, and some efforts made to balance them (Dumer & Shabunov, 2001); that KO codes learn such a balancing scheme purely from data is, perhaps, remarkable.

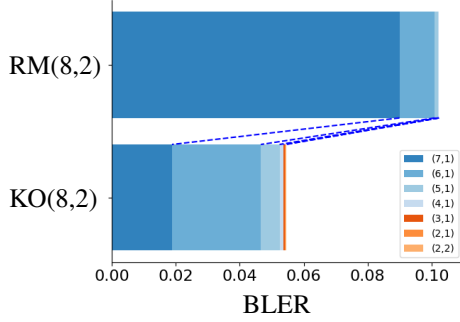


Figure 6. Separating each sub-code contribution in the KO(8,2) decoder and the RM(8,2) decoder reveals that KO(8,2) improves in the total BLER by balancing the contributions more evenly over the sub-codes.

4.3. Robustness to non-AWGN channels

As the environment changes dynamically in real world channels, robustness is crucial in practice. We therefore test the KO code under canonical channel models and demonstrate robustness, i.e., the ability of a code trained on AWGN to perform well under a different channel *without retraining*. It is well known that Gaussian noise is the worst case noise among all noise with the same variance (Lapidoth, 1996; Shannon, 1948) when an optimal decoder is used, which might take an exponential time. When decoded with efficient decoders, as we do with both RM and KO codes, catastrophic failures have been reported in the case of Turbo decoders (Kim et al., 2018). We show that both RM codes and KO codes are robust and maintain their gains over RM codes as the channels vary.

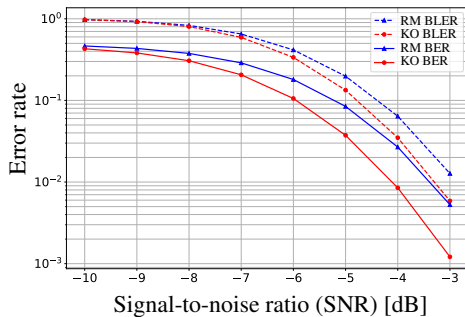


Figure 7. KO(8,2) trained on AWGN is robust when tested on a fast fading channel and maintains a significant gain over RM(8,2).

We first test on a *Rayleigh fast fading channel*, defined as

$y_i = a_i x_i + n_i$, where x_i is the transmitted symbol, y_i is the received symbol, $n_i \sim \mathcal{N}(0, \sigma^2)$ is the additive Gaussian noise, and a is from a Rayleigh distribution with the variance of a chosen as $\mathbb{E}[a_i^2] = 1$.

We next test on a bursty channel, defined as $y_i = x_i + n_i + w_i$, where x_i is the input symbol, y_i is the received symbol, $n_i \sim \mathcal{N}(0, \sigma^2)$ is the additive Gaussian noise, and $w_i \sim \mathcal{N}(0, \sigma_b^2)$ with probability ρ and $w_i = 0$ with probability $1 - \rho$. In the experiment, we choose $\rho = 0.1$ and $\sigma_b = \sqrt{2}\sigma$.

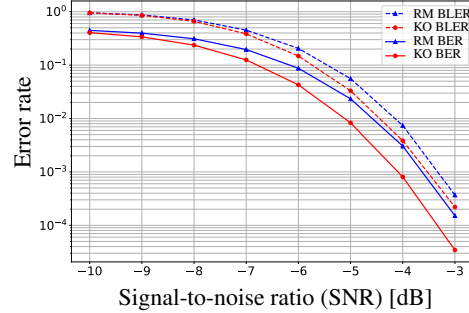


Figure 8. KO(8,2) trained on AWGN is robust when tested on a bursty channel and maintains a significant gain over RM(8,2).

4.4. Complexity of KO decoding

Ultra-Reliable Low Latency Communication (URLLC) is increasingly required for modern applications including vehicular communication, virtual reality, and remote robotics (Sybis et al., 2016; Jiang et al., 2020). In general, a $KO(m, r)$ code requires $O(n \log n)$ operations to decode which is the same as the efficient Dumer's decoder for an $RM(m, r)$ code, where $n = 2^m$ is the block length. More precisely, the decoder for $RM(8, 2)$ requires 11268 operations whereas $KO(8, 2)$ requires 550644 operations which we did not try to optimize for this project. With recent model compression techniques, we believe this can be decreased to be comparable with the Dumer's decoder.

5. KO codes improve upon Polar codes

Results from Section 4 demonstrate that our KO codes significantly improve upon RM codes on a variety of benchmarks. Here, we focus on a different family of capacity-achieving landmark codes: *Polar codes* (Arikan, 2009).

Polar and RM codes are closely related, especially from an encoding point of view. The generator matrices of both codes come from the same parent square matrix by following different row selection rules. More precisely, consider an $RM(m, r)$ code that has code dimension $k = \sum_{i=0}^r \binom{m}{i}$ and blocklength $n = 2^m$. Its encoding generator matrix is obtained by picking the k rows of the square ma-

trix $\mathbf{G}_{n \times n} := \begin{bmatrix} 0 & 1 \\ 1 & 1 \end{bmatrix}^{\otimes m}$ that have the largest Hamming weights (i.e., Hamming weight of at least 2^{m-r}), where $[\cdot]^{\otimes m}$ denotes the m -th Kronecker power. The Polar encoder, on the other hand, picks the rows of $\mathbf{G}_{n \times n}$ that have the lowest Bhattacharyya parameter (Arıkan, 2009).

In view of the Kronecker structure inherent to the parent matrix $\mathbf{G}_{n \times n}$, the Polar encoder can be alternatively represented by a computation graph, which we refer to as its *Plotkin tree*. Specifically, the Plotkin tree for a Polar code is represented by a complete binary tree (the recursive Kronecker product), where a set of leaves are frozen to zero (row-selection). This Plotkin tree structure enables a matching efficient decoder for Polar codes, called the *Successive Cancellation* (SC). The SC decoding algorithm is similar to Dumer’s decoding for RM codes. More importantly, the SC decoder is the state-of-the-art decoding algorithm to decode Polar codes and is an important component towards them achieving capacity. Hence Polar codes, can be completely characterized by their corresponding Plotkin trees.

The Plotkin tree viewpoint of Polar codes enables us to build new network architectures. In other words, capitalizing on the structure of Polar Plotkin trees, we design a new family of KO codes to strictly improve upon them. Further, the KO encoder and decoder can be trained in an end-to-end manner using variants of stochastic gradient descent. We defer these details to Appendix A.

In Figure 9, we compare the performance our KO code with its competing Polar(64, 7) code, i.e., code dimension $k = 7$ and block length $n = 64$, in terms of BER. Figure 9 highlights that our KO code achieves significant gains over Polar(64, 7) on a wide range of SNRs. In particular, we obtain a gain of almost 0.7 dB compared to that of Polar at the BER 10^{-4} . For comparison we also plot the performance of both codes with the optimal MAP decoding. We observe that the BER curve of our KO decoder, unlike the SC decoder, almost matches that of the MAP decoder, convincingly demonstrating its optimality.

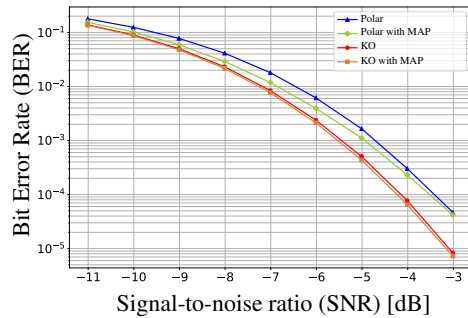


Figure 9. Neural network based KO code improves upon the Polar(64, 7) code when trained on AWGN channel. KO decoder also matches the optimal MAP decoder.

We also observe similar improvements for BLER (Figure 11, Appendix A). This successful case study with training KO (encoder, decoder) pairs further demonstrates that our novel neural architectures seamlessly generalize to codes with an underlying Kronecker product structure.

6. Related work

There is tremendous interest in the coding theory community to incorporate deep learning methods. In the context of channel coding, the bulk of the works focus on decoding known linear codes using data-driven neural decoders (Nachmani et al., 2016; O’shea & Hoydis, 2017; Dörner et al., 2017; Nachmani et al., 2018; Kim et al., 2018; Jiang et al., 2019a); even here, most works have limited themselves to small block lengths due to the difficulty in generalization (for instance, even when nearly 90% of the codewords of a rate 1/2 Polar code over 8 information bits are exposed to the neural decoder (Gruber et al., 2017)).

On the other hand, very few works in the literature focus on discovering *both* encoders and decoders; the few which do, operate at very small block lengths (O’shea et al., 2016; O’shea & Hoydis, 2017). One of the major challenges here is to jointly train the (encoder, decoder) pairs without getting stuck in local optima as the losses are non-convex. In (Jiang et al., 2019b), the authors employ clever training tricks to learn a novel autoencoder based codes that outperform the classical Turbo codes, which are sequential in nature. In contrast, here we focus on the generalizations of the Kronecker operation that underpins the RM and Polar family.

RM and Polar codes have seen active research, especially on improving decoding using neural networks: (Xu et al., 2017; Cammerer et al., 2017; Doan et al., 2018; Carpi et al., 2019). (Ebada et al., 2019) proposes a method to learn the frozen indices of a Polar code together with the weights in the belief propagation (BP) factor graph that improves upon the classical BP decoding. However, BP decoder is sub-optimal for Polar codes; in comparison, we strictly improve upon their state of the art decoding (Figure 9).

7. Conclusion

We introduce KO codes that generalize the recursive Kronecker operation crucial in designing RM and Polar codes. Using the computation tree (known as a Plotkin tree) of these classical codes as a skeleton, we propose a novel neural network architecture tailored for communication. Training over AWGN, we discover the first family of *non-linear* codes that significantly outperform the baseline the KO code was built upon. The pairwise distance profile reveals that KO code combines the analytical structure of algebraic codes with the random structure of the celebrated random Gaussian codes.

References

- Abbe, E., Shpilka, A., and Wigderson, A. Reed-muller codes for random erasures and errors. *IEEE Transactions on Information Theory*, 61(10):5229–5252, 2015.
- Abbe, E., Shpilka, A., and Ye, M. Reed-muller codes: Theory and algorithms, 2020.
- Alon, N., Kaufman, T., Krivelevich, M., Litsyn, S., and Ron, D. Testing reed-muller codes. *IEEE Transactions on Information Theory*, 51(11):4032–4039, 2005.
- Arikan, E. Channel polarization: A method for constructing capacity-achieving codes for symmetric binary-input memoryless channels. *IEEE Transactions on information Theory*, 55(7):3051–3073, 2009.
- Cammerer, S., Gruber, T., Hoydis, J., and Ten Brink, S. Scaling deep learning-based decoding of polar codes via partitioning. In *GLOBECOM 2017-2017 IEEE global communications conference*, pp. 1–6. IEEE, 2017.
- Carpi, F., Häger, C., Martalò, M., Raheli, R., and Pfister, H. D. Reinforcement learning for channel coding: Learned bit-flipping decoding. In *2019 57th Annual Allerton Conference on Communication, Control, and Computing (Allerton)*, pp. 922–929. IEEE, 2019.
- Doan, N., Hashemi, S. A., and Gross, W. J. Neural successive cancellation decoding of polar codes. In *2018 IEEE 19th international workshop on signal processing advances in wireless communications (SPAWC)*, pp. 1–5. IEEE, 2018.
- Dörner, S., Cammerer, S., Hoydis, J., and Ten Brink, S. Deep learning based communication over the air. *IEEE Journal of Selected Topics in Signal Processing*, 12(1):132–143, 2017.
- Dumer, I. Recursive decoding and its performance for low-rate reed-muller codes. *IEEE Transactions on Information Theory*, 50(5):811–823, 2004.
- Dumer, I. Soft-decision decoding of reed-muller codes: a simplified algorithm. *IEEE transactions on information theory*, 52(3):954–963, 2006.
- Dumer, I. and Shabunov, K. Near-optimum decoding for subcodes of reed-muller codes. In *Proceedings. 2001 IEEE International Symposium on Information Theory*, pp. 329. IEEE, 2001.
- Dumer, I. and Shabunov, K. Soft-decision decoding of reed-muller codes: recursive lists. *IEEE Transactions on information theory*, 52(3):1260–1266, 2006.
- Ebada, M., Cammerer, S., Elkelesh, A., and ten Brink, S. Deep learning-based polar code design. In *2019 57th Annual Allerton Conference on Communication, Control, and Computing (Allerton)*, pp. 177–183. IEEE, 2019.
- Gruber, T., Cammerer, S., Hoydis, J., and ten Brink, S. On deep learning-based channel decoding. In *2017 51st Annual Conference on Information Sciences and Systems (CISS)*, pp. 1–6. IEEE, 2017.
- Jiang, Y., Kannan, S., Kim, H., Oh, S., Asnani, H., and Viswanath, P. Deepturbo: Deep turbo decoder. In *2019 IEEE 20th International Workshop on Signal Processing Advances in Wireless Communications (SPAWC)*, pp. 1–5. IEEE, 2019a.
- Jiang, Y., Kim, H., Asnani, H., Kannan, S., Oh, S., and Viswanath, P. Turbo autoencoder: Deep learning based channel codes for point-to-point communication channels. In *Advances in Neural Information Processing Systems*, pp. 2758–2768, 2019b.
- Jiang, Y., Kim, H., Asnani, H., Kannan, S., Oh, S., and Viswanath, P. Learn codes: Inventing low-latency codes via recurrent neural networks. *IEEE Journal on Selected Areas in Information Theory*, 2020.
- Kaufman, T., Lovett, S., and Porat, E. Weight distribution and list-decoding size of reed-muller codes. *IEEE transactions on information theory*, 58(5):2689–2696, 2012.
- Kim, H., Jiang, Y., Rana, R., Kannan, S., Oh, S., and Viswanath, P. Communication algorithms via deep learning. *arXiv preprint arXiv:1805.09317*, 2018.
- Kim, H., Oh, S., and Viswanath, P. Physical layer communication via deep learning. *IEEE Journal on Selected Areas in Information Theory*, 2020.
- Kudekar, S., Kumar, S., Mondelli, M., Pfister, H. D., Şaşoğlu, E., and Urbanke, R. L. Reed-muller codes achieve capacity on erasure channels. *IEEE Transactions on information theory*, 63(7):4298–4316, 2017.
- Lapidoth, A. Nearest neighbor decoding for additive non-gaussian noise channels. *IEEE Transactions on Information Theory*, 42(5):1520–1529, 1996.
- Ma, Z., Xiao, M., Xiao, Y., Pang, Z., Poor, H. V., and Vucetic, B. High-reliability and low-latency wireless communication for internet of things: challenges, fundamentals, and enabling technologies. *IEEE Internet of Things Journal*, 6(5):7946–7970, 2019.
- Nachmani, E., Be’ery, Y., and Burshtein, D. Learning to decode linear codes using deep learning. In *2016 54th Annual Allerton Conference on Communication, Control, and Computing (Allerton)*, pp. 341–346. IEEE, 2016.

- Nachmani, E., Marciano, E., Lugosch, L., Gross, W. J., Burshtein, D., and Be'ery, Y. Deep learning methods for improved decoding of linear codes. *IEEE Journal of Selected Topics in Signal Processing*, 12(1):119–131, 2018.
- O'Shea, T. J., Karra, K., and Clancy, T. C. Learning to communicate: Channel auto-encoders, domain specific regularizers, and attention. In *2016 IEEE International Symposium on Signal Processing and Information Technology (ISSPIT)*, pp. 223–228. IEEE, 2016.
- O'shea, T. and Hoydis, J. An introduction to deep learning for the physical layer. *IEEE Transactions on Cognitive Communications and Networking*, 3(4):563–575, 2017.
- Plotkin, M. Binary codes with specified minimum distance. *IRE Transactions on Information Theory*, 6(4):445–450, 1960.
- Polyanskiy, Y., Poor, H. V., and Verdú, S. Channel coding rate in the finite blocklength regime. *IEEE Transactions on Information Theory*, 56(5):2307–2359, 2010.
- Reed, I. A class of multiple-error-correcting codes and the decoding scheme. *Transactions of the IRE Professional Group on Information Theory*, 4(4):38–49, 1954.
- Richardson, T. and Urbanke, R. *Modern coding theory*. Cambridge University Press, 2008.
- Sason, I. and Shamai, S. Performance analysis of linear codes under maximum-likelihood decoding: A tutorial. 2006.
- Sberlo, O. and Shpilka, A. On the performance of reed-muller codes with respect to random errors and erasures. In *Proceedings of the Fourteenth Annual ACM-SIAM Symposium on Discrete Algorithms*, pp. 1357–1376. SIAM, 2020.
- Senior, A. W., Evans, R., Jumper, J., Kirkpatrick, J., Sifre, L., Green, T., Qin, C., Žídek, A., Nelson, A. W., Bridgland, A., et al. Protein structure prediction using multiple deep neural networks in the 13th critical assessment of protein structure prediction (casp13). *Proteins: Structure, Function, and Bioinformatics*, 87(12):1141–1148, 2019.
- Shannon, C. E. A mathematical theory of communication. *The Bell system technical journal*, 27(3):379–423, 1948.
- Silver, D., Hubert, T., Schrittwieser, J., Antonoglou, I., Lai, M., Guez, A., Lanctot, M., Sifre, L., Kumaran, D., Graepel, T., et al. A general reinforcement learning algorithm that masters chess, shogi, and go through self-play. *Science*, 362(6419):1140–1144, 2018.
- Sybis, M., Wesolowski, K., Jayasinghe, K., Venkatasubramanian, V., and Vukadinovic, V. Channel coding for ultra-reliable low-latency communication in 5g systems. In *2016 IEEE 84th vehicular technology conference (VTC-Fall)*, pp. 1–5. IEEE, 2016.
- Udrescu, S.-M. and Tegmark, M. Ai feynman: A physics-inspired method for symbolic regression. *Science Advances*, 6(16):eaay2631, 2020.
- Welling, M. Neural augmentation in wireless communication, 2020.
- Xu, W., Wu, Z., Ueng, Y.-L., You, X., and Zhang, C. Improved polar decoder based on deep learning. In *2017 IEEE International workshop on signal processing systems (SiPS)*, pp. 1–6. IEEE, 2017.

Appendix

A. Plotkin tree of Polar(64, 7) code

The Plotkin decomposition of Polar(64, 7) code is schematically shown in Figure 10 through a tree diagram. Additionally, the Plotkin encoding for this code is depicted in blue color assuming (u_1, \dots, u_7) as the information bits. Compared to the RM counterpart, i.e., RM(6, 1), this code has $\mathbf{v}_5 = (0, \dots, 0)_{1 \times 32}$ instead of an RM(5, 0) at the topmost left branch. In other words, the Polar encoder freezes all the first 32 bits to zero while the RM encoder repeats one of the seven information bits 32 times in the first half of the blocklength. Additionally, the Polar(64, 7) code has a full-rate RM(1, 1) code instead of rate-half RM(1, 0) for \mathbf{v}_1 . Note that the middle (n, k) codes (e.g., the (32, 7) code) are not necessarily (n, k) Polar codes given that the information bit indices might be different. However, they are still Plotkin codes following the decomposition $(\mathbf{u}, \mathbf{u} \oplus \mathbf{v})$, where \mathbf{u} and \mathbf{v} are the codes at the right and left branches, respectively.

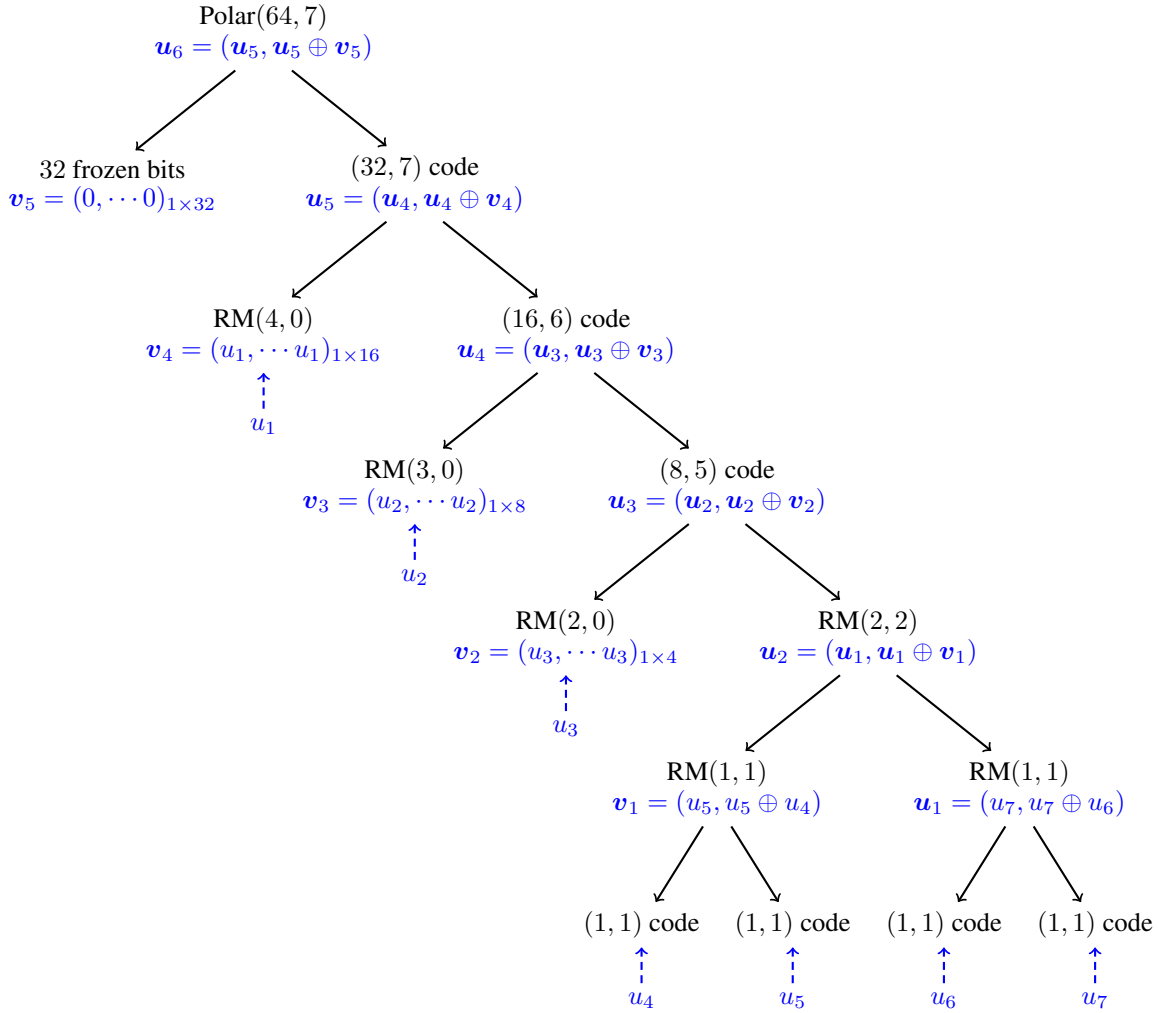


Figure 10. Plotkin tree representation of Polar(64, 7) code. The middle (n, k) codes (e.g., the (32, 7) code) are not necessarily (n, k) Polar codes (the information bit indices might be different). However, they are still Plotkin codes following the decomposition $(\mathbf{u}, \mathbf{u} \oplus \mathbf{v})$, where \mathbf{u} and \mathbf{v} are the codes at the right and left branches, respectively. The Plotkin encoding for this code is also depicted in blue color assuming (u_1, \dots, u_7) as the information bits.

Given the encoding tree diagram, during the construction of the neural encoder we do not use a neural network at the topmost level, rather we simply concatenate the code at the right branch with itself. This intuition for the encoding of Polar codes based on the above tree diagram, i.e., $\mathbf{u}_6 = (\mathbf{u}_5, \mathbf{u}_5 \oplus \mathbf{u}_4)$, seems to be helpful in training the neural encoder. Additionally, during the construction of the neural decoder, we first add the first half of the corrupted codewords to their second half to

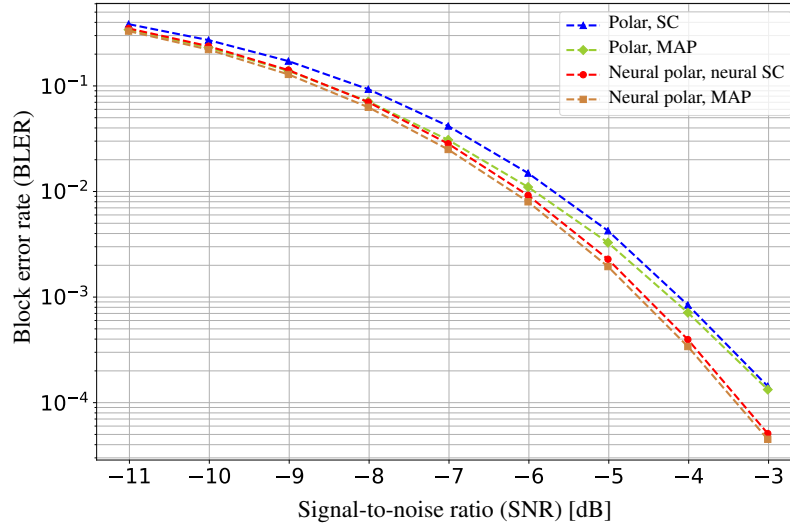


Figure 11. BLER performance of Polar(64, 7) code.

obtain an updated version of the corrupted codewords to work with from the topmost right branch. This intuition, which also comes from the successive cancellation decoding of Polar codes given that the topmost left branch is all frozen bits, significantly contributes in successfully training the neural decoder for the neural Polar(64, 7) code.

Figure 11 shows the BLER performance of the considered Polar code detailed in Section 5. Similar to the BER performance analyzed in Figure 9, the neural Polar encoder is able to significantly improve the BLER performance. For example, almost 0.5 dB improvement is achieved for the BLER of the MAP decoder with our neural encoder. Additionally, the close performance of our neural SC decoder to that of the MAP decoder for the neural Polar code, once again, confirms the efficiency of our neural decoder.

B. Discussion

B.1. Real-valued codewords vs. binary codewords

In practice, wireless communication protocols often utilize binary codes. This is mainly because the entire digital communication paradigm is built upon expressing the information in terms of binary bits (Shannon, 1948). Furthermore, system hardware for transceivers essentially consists of binary logic gates as the building blocks making binary encoding and decoding a natural choice. We discretize the output of our KO encoder to output a binary valued codeword $\mathbf{x} \in \{\pm 1\}^n$, which we denote by KO-b(8,2). KO-b(8,2) only slightly improves over the RM(8,2), suggesting that searching over the larger space of real-valued codewords is critical. Further, for KO-b codes, the Gaussian-like structure of trained codewords is destroyed and pairwise distribution falls back to that of RM codes (Figure 5 green).

B.2. Computational complexity of KO codes

Ultra-Reliable Low Latency Communication (URLLC) is increasingly required for modern applications including vehicular communication, virtual reality, and remote robotics (Sybis et al., 2016; Jiang et al., 2020). In general, a KO(m, r) code requires $O(n \log n)$ operations to decode which is the same as the efficient Dumer's decoder for a RM(m, r) code, where $n = 2^m$ is the block length. More precisely, the decoder for RM(8, 2) requires 11268 operations whereas KO(8, 2) requires 550644 operations which we did not try to optimize for this project. With recent model compression techniques, we believe this can be decreased to be comparable with the Dumer's decoder.

C. Plotkin construction

Plotkin (1960) proposed this scheme in order to combine two codes of smaller code lengths and construct a larger code with the following properties. It is relatively easy to construct a code with either a high rate but a small distance (such as sending the raw information bits directly) or a large distance but a low rate (such as repeating each bit multiple times). Plotkin construction combines such two codes of rates $\rho_u > \rho_v$ and distances $d_u < d_v$, to design a larger block length code satisfying rate $\rho = (\rho_u + \rho_v)/2$ and distance $\min\{2d_u, d_v\}$. This significantly improves upon a simple time-sharing of those codes, which achieves the same rate but distance only $\min\{d_u, d_v\}$.

Following the standard convention, we fix the leaves in the Plotkin tree of a first order $\text{RM}(m, 1)$ code to be zeroth order RM codes and the full-rate $\text{RM}(1, 1)$ code. On the other hand, a second order $\text{RM}(m, 2)$ code contains the first order RM codes and the full-rate $\text{RM}(2, 2)$ as its leaves.

D. $\text{KO}(8, 2)$: Architecture and training

As highlighted in §4, our KO codes improve upon RM codes significantly on a variety of benchmarks. We present the architectures of the $\text{KO}(8, 2)$ encoder and the $\text{KO}(8, 2)$ decoder, and their joint training methodology that are crucial for this superior performance. Figure 4 illustrates the $\text{KO}(8, 2)$ code.

D.1. $\text{KO}(8, 2)$ encoder

$\text{KO}(8, 2)$ encoder inherits the same Plotkin tree structure as that of the second order $\text{RM}(8, 2)$ code and thus RM codes of first order and the second order $\text{RM}(2, 2)$ code constitute the leaves of this tree, as highlighted in Figure 4a. On the other hand, a critical component of our $\text{KO}(8, 2)$ encoder is a set of encoding neural networks $g_\theta = \{g_1, \dots, g_6\}$ that strictly generalize the Plotkin mapping. In other words, we associate a neural network $g_i \in g_\theta$ to each internal node i of this tree. If \mathbf{v} and \mathbf{u} denote the codewords arriving from left and right branches at this node, we combine them non-linearly via the operation $(\mathbf{u}, \mathbf{v}) \mapsto (\mathbf{u}, g_i(\mathbf{u}, \mathbf{v}))$.

We carefully parametrize each $g_i \in g_\theta$ so that they generalize the classical Plotkin map $\text{Plotkin}(\mathbf{u}, \mathbf{v}) = \mathbf{u} \oplus \mathbf{v}$. In particular, we represent it as $g_i(\mathbf{u}, \mathbf{v}) = \tilde{g}_i(\mathbf{u}, \mathbf{v}) + \mathbf{u} \oplus \mathbf{v}$, where \tilde{g}_i is a 3-hidden layer feedforward network of appropriate input and output dimensions. This clever parametrization, in addition to allowing for general non-linearities g_i to be learnt at each node, in turn allows for a much richer and broader class of non-linear encoders and codes to be discovered on a whole. Similar skip-like ideas have been successfully used in the literature though in a different context of learning decoders (Welling, 2020). On the other hand, we exploit these ideas for both encoders and decoders which further contribute to significant gains over RM codes.

From an encoding perspective, recall that the $\text{KO}(8, 2)$ code has code dimension $k = 37$ and block length $n = 256$. Suppose we wish to transmit a set of 37 message bits denoted as $\mathbf{m} = (\mathbf{m}_{(2,2)}, \mathbf{m}_{(2,1)}, \dots, \mathbf{m}_{(7,1)})$ through our $\text{KO}(8, 2)$ encoder. We first encode the block of four message bits $\mathbf{m}_{(2,2)}$ into a $\text{RM}(2, 2)$ codeword $\mathbf{c}_{(2,2)}$ using its corresponding encoder at the bottom most leaf of the Plotkin tree. Similarly we encode the next three message bits $\mathbf{m}_{(2,1)}$ into an $\text{RM}(2, 1)$ codeword $\mathbf{c}_{(2,1)}$. These codewords are then non-linearly combined by the neural network g_2 into a codeword $\mathbf{c}_{(3,2)} = (\mathbf{c}_{(2,2)}, g_2(\mathbf{c}_{(2,2)}, \mathbf{c}_{(2,1)})) \in \mathbb{R}^8$. The codeword $\mathbf{c}_{(3,2)}$ is similarly combined with its corresponding left codeword and this procedure is thus recursively carried out till we reach the top most node of the tree which outputs the codeword $\mathbf{c}_{(8,2)} \in \mathbb{R}^{256}$. Finally we obtain the unit-norm $\text{KO}(8, 2)$ codeword \mathbf{x} by normalizing $\mathbf{c}_{(8,2)}$, i.e. $\mathbf{x} = \mathbf{c}_{(8,2)} / \|\mathbf{c}_{(8,2)}\|_2$. Figure 12 illustrates this encoding procedure.

Note that the map of encoding the message bits \mathbf{m} into the codeword \mathbf{x} , i.e. $\mathbf{x} = g_\theta(\mathbf{m})$, is differentiable with respect to θ since all the underlying operations at each node of the Plotkin tree are differentiable.

D.2. $\text{KO}(8, 2)$ -decoder

Capitalizing on the recursive structure of the encoder, the $\text{KO}(8, 2)$ decoder decodes the message bits from top to bottom, similar in style to Dumer’s decoding in §2. More specifically, at any internal node of the tree we first decode the message bits along its left branch which we utilize to decode that of the right branch and this procedure is carried out recursively till all the bits are recovered.

Similar to the encoding neural networks g_θ , an important aspect of our $\text{KO}(8, 2)$ decoder is a set of decoding neural networks

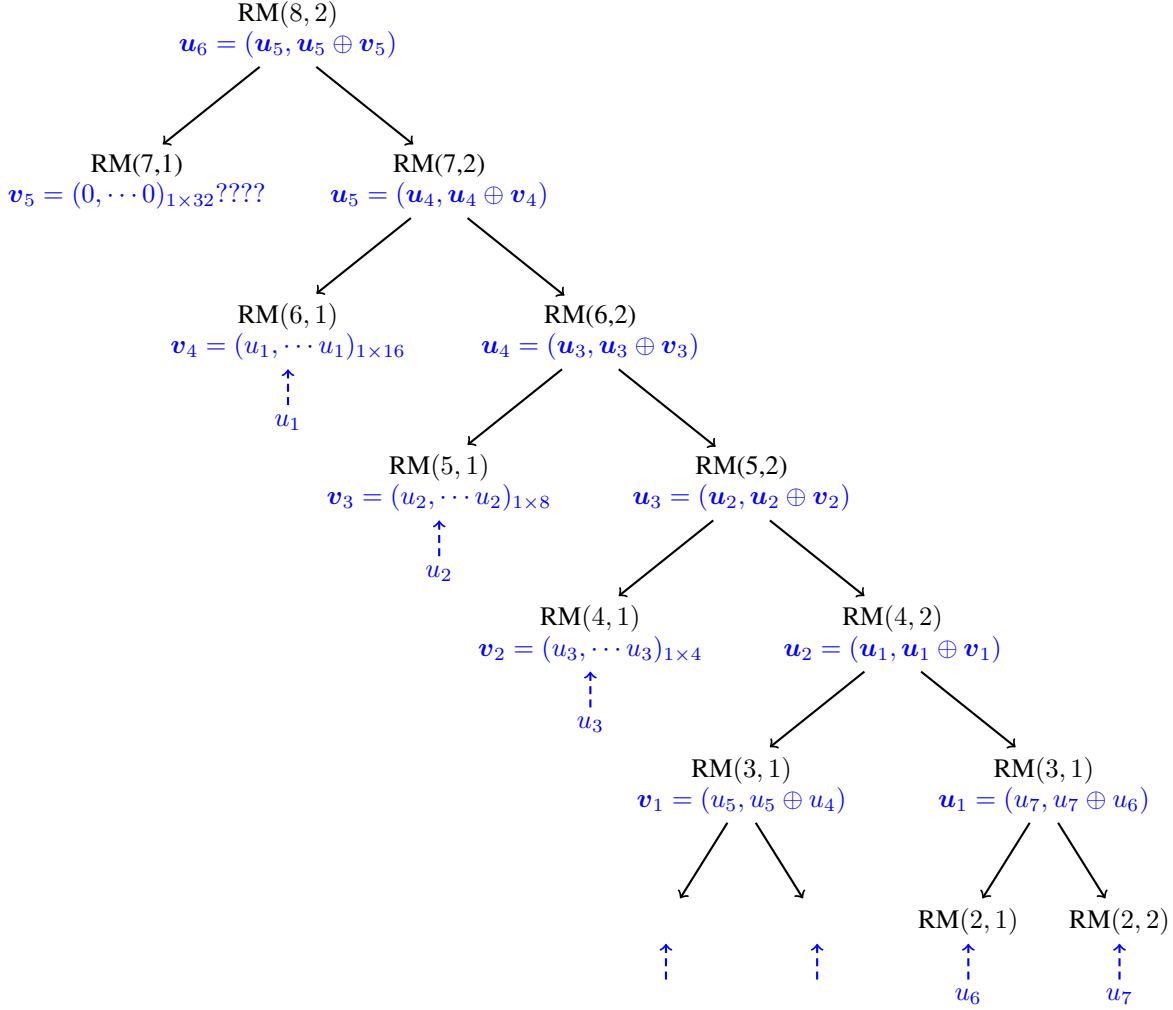


Figure 12. Plotkin tree representation of RM(8, 2) code. [Sewoong: needs to be revised]

$f_\phi = \{f_1, f_2, \dots, f_{11}, f_{12}\}$. Here each f_{2i-1} corresponds to a left branch in the tree whereas f_{2i} corresponds to a right branch. Thus for any node i in the tree, its decoding neural networks (f_{2i-1}, f_{2i}) can be interpreted as matching decoders for the corresponding encoding network g_i . While g_i encodes the left and right codewords arriving at the node, f_{2i-1} and f_{2i} estimate these codewords using a proxy for their LLR vector. Furthermore, allowing for a strict generalization over Dumer's decoding, we again carefully parametrize each (f_{2i-1}, f_{2i}) so that they recover the classical Dumer's decoding as a special case. We refer to [Appendix something](#) for more details.

At the decoder suppose we receive a noisy codeword $\mathbf{y} \in \mathbb{R}^{256}$ upon transmission of the actual codeword $\mathbf{x} \in \mathbb{R}^{256}$ along the channel. In view of the encoding structure at the root of the tree, we first pass \mathbf{y} along the left branch NN f_1 to obtain a feature vector $f_1(\mathbf{y})$. This feature can be thought of the LLR vector for the corresponding RM(7, 1) codeword. Subsequently, the Soft-MAP decoder transforms this feature vector into an LLR vector for the message bits, i.e. $\mathbf{L}_{(7,1)} = \text{SoftMAP}(f_1(\mathbf{y}))$. Note that the message bits $\mathbf{m}_{(7,1)}$ can be easily estimated from the sign of $\mathbf{L}_{(7,1)}$. Similarly the feature vector for the right codeword can be computed using the right decoder f_2 , i.e. $\mathbf{L}_{(7,2)} = f_2(\mathbf{y}, \mathbf{L}_{(7,1)})$. Utilizing this feature $\mathbf{L}_{(7,2)}$ the decoding procedure is thus recursively carried out till we compute the LLRs for all the remaining message bits $\mathbf{m}_{(6,1)}, \dots, \mathbf{m}_{(2,2)}$. Finally we obtain the full LLR vector $\mathbf{L} = (\mathbf{L}_{(7,1)}, \dots, \mathbf{L}_{(2,2)})$ corresponding to the message bits \mathbf{m} . A simple transformation, $\sigma(\mathbf{L})$, further yields the probability of each of these message bits being zero.

Note that we pass the soft-information of LLR vectors, i.e. $\mathbf{L}_{(7,1)}, \mathbf{L}_{(6,1)}$, etc., instead of the actual decoded message bits down the tree during the decoding procedure. This is done to ensure that the decoding map $\mathbf{L} = f_\phi(\mathbf{y})$ is fully differentiable,

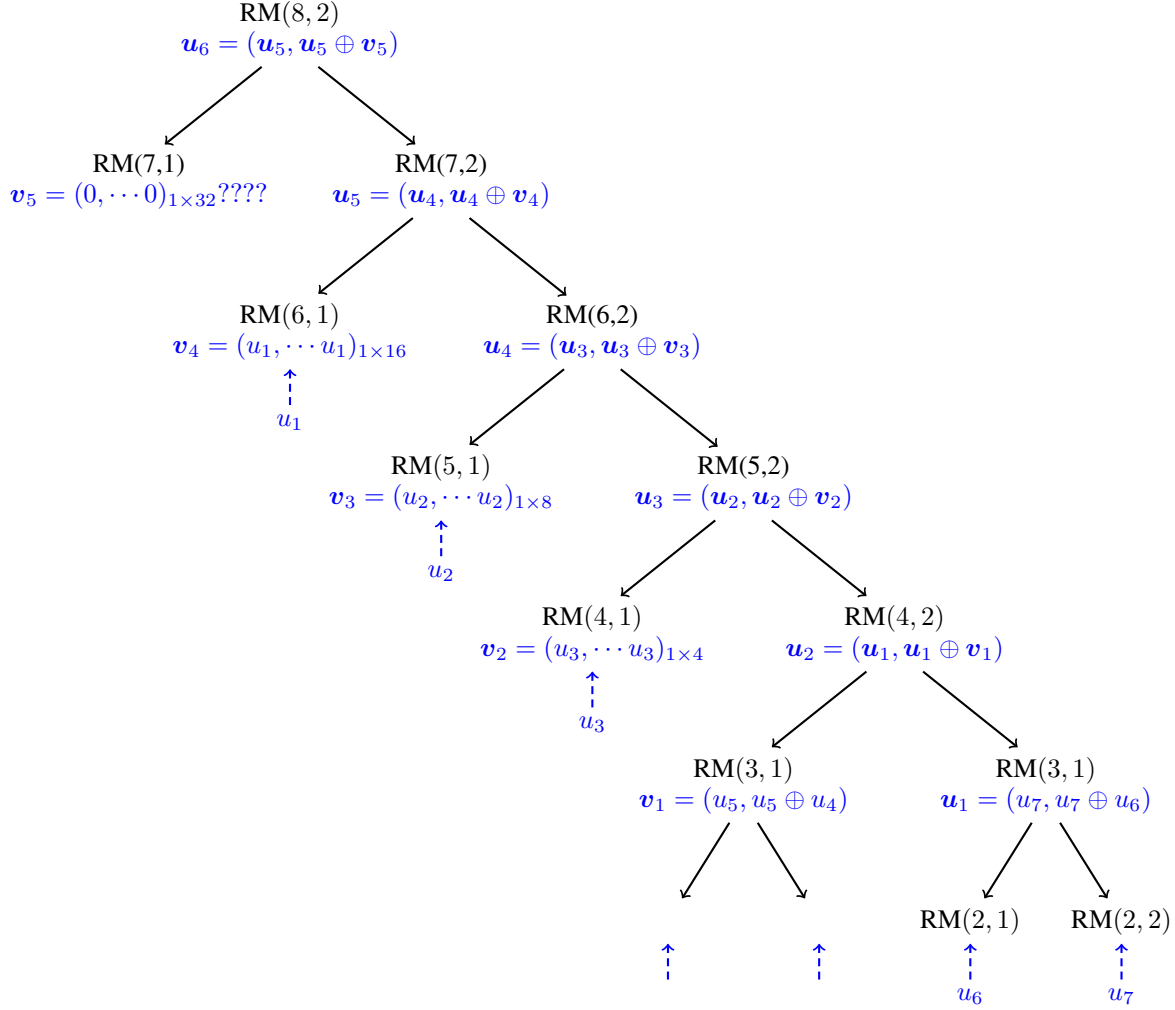


Figure 13. Plotkin tree representation of KO(8, 2) code. [Sewoong: needs to be revised]

which further ensures a differentiable loss for training the parameters (θ, ϕ) .

D.3. Training

Recall that we have the following flow diagram from encoder till the decoder when we transmit the message bits m : $m \xrightarrow{g_\theta} x \xrightarrow{\text{Channel}} y \xrightarrow{f_\phi} L \xrightarrow{\sigma(\cdot)} \sigma(L)$. In view of this, we define an end-to-end differentiable cross entropy loss function to train the parameters (θ, ϕ) , i.e.

$$L(\theta, \phi) = \sum_{j \in \mathcal{L}} m_j \log(1 - \sigma(L_j)) + (1 - m_j) \log \sigma(L_j),$$

where $\mathcal{L} = \{(7, 1), \dots, (2, 2)\}$ denotes the set of leaf indices in the tree. Finally we run [Algorithm 3](#) to train the parameters (θ, ϕ) via gradient descent.

E. Efficient decoder vs. MAP decoder

Soft MAP decoder. [Sewoong: Vahid: can you explain soft-MAP decoder in detail here?]

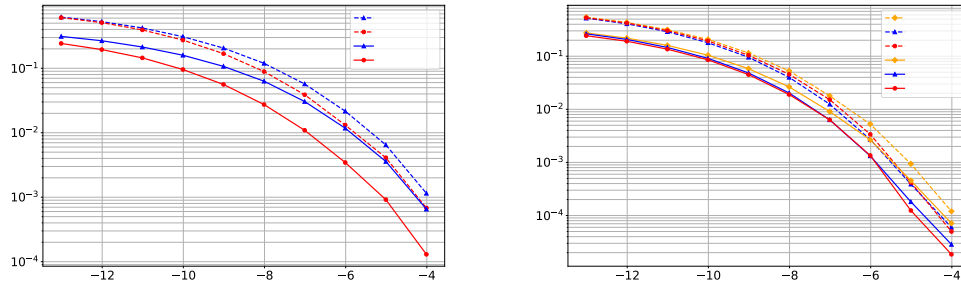


Figure 14. BER /SNR KO(6,1), RM(6,1) dumer decoding (left) and BER /SNR KO(6,1), RM(6,1) MAP decoding (right)

Figure 15. Histogram of pariwise distances KO(6,1), RM(6,1) MAP decoding

F. Experimental details

What is the loss

What is the architecture (for KO(8,2))

optimization

learning rate